

# Tunable terahertz filter based on alternative liquid crystal layers and metallic slats

Shijun Ge (葛士军)<sup>1</sup>, Jiachen Liu (刘嘉晨)<sup>1</sup>, Peng Chen (陈鹏)<sup>1</sup>, Wei Hu (胡伟)<sup>1,\*</sup>,  
and Yanqing Lu (陆延青)<sup>1,2</sup>

<sup>1</sup>National Laboratory of Solid State Microstructures and College of Engineering and Applied Sciences,  
Nanjing University, Nanjing 210093, China

<sup>2</sup>Email: yqlu@nju.edu.cn

\*Corresponding author: huwei@nju.edu.cn

Received September 15, 2015; accepted October 27, 2015; posted online December 15, 2015

We propose and demonstrate a pseudo Fabry–Pérot filter in the terahertz frequency range of 0.1–0.5 THz. It consists of alternative liquid crystal layers and metallic slats. Separate sharp resonant peaks are shown in the simulated transmission spectra, and their positions shift toward higher frequencies when the refractive index of liquid crystal decreases. The measured transmission spectra are consistent with corresponding simulations. Via thermally tuning the refractive index of the filled liquid crystal, the resonant transmission frequencies shift accordingly. The work supplies a novel design for tunable terahertz filters, which would play important roles in terahertz imaging, sensing, high speed communication, and security applications.

OCIS codes: 040.2235, 120.2230, 120.2440, 160.3710.

doi: 10.3788/COL201513.120401.

A terahertz (THz) wave, which is typically defined as electromagnetic wave in the frequency range of 0.1–10 THz, falls in the gap between photonics and electronics. It exhibits many unique characteristics and offers great potentials in security screening, nondestructive evaluation and high-speed wireless communication<sup>[1–4]</sup>. The past two decades have witnessed the impressive progress of THz technology. However, compared with the well-established sources and detectors<sup>[1,2,5,6]</sup>, research on passive functional components, which are essential to manipulate THz waves, are still in the ascendant<sup>[7,8]</sup>. Like their optical counterparts, THz components, such as THz phase shifter<sup>[9]</sup>, wave plates<sup>[10,11]</sup>, polarization controllers<sup>[12]</sup>, and filters<sup>[13,14]</sup> are in high demand to handle THz waves as well, especially tunable ones.

Among these components, filters have drawn special attention due to their functions in selectively transmitting waves in particular frequency ranges. Photonic crystals<sup>[15]</sup>, metallic micron-sized hole arrays<sup>[16]</sup>, and pillared lattices<sup>[7]</sup> were demonstrated as bandpass filters. All of these filters work only for given wavelengths or specific THz bands, namely, they are not tunable, limiting their applications. To realize tunable filters, a mixed-type I/type II GaAs/AlAs multiple quantum well structure was introduced and tuned by optical injection<sup>[17]</sup>. By doping SrTiO<sub>3</sub> into periodic alternating layers of quartz and high-permittivity ceramic, Nemeč *et al.* tuned a stop band from 0.185 THz down to 0.100 THz through temperature control<sup>[18]</sup>. Thanks to the broadband tunability of liquid crystals (LCs) whose refractive index can be easily controlled by an external field (e.g., electric, magnetic, and thermal fields)<sup>[19,20]</sup>, corresponding components have attracted growing interest<sup>[13,21,22]</sup>. Pan's group reported tunable Lyot filters and Solc filters via magnetically tuning LC phase

retarders<sup>[13,14]</sup>. Vieweg *et al.* demonstrated a tunable THz Notch filter via electrically controlling the birefringence of LCs<sup>[23]</sup>. A Fabry–Pérot (FP) filter is another useful category that has been widely used from the visible to microwave bands<sup>[24–27]</sup>. Attempts toward THz FP filters are quite meaningful.

Here, we propose a design of a pseudo FP THz filter. It consists of alternative LC layers and metallic slats. After simulation optimization and further taking practical fabrication into account, the structure with chosen parameters is schematically illustrated in Fig. 1. Thirty-two stainless steel slats are stacked together and separated with Mylar film. The dimensions of the slats are length  $L = 15.0$  mm, width  $T = 2.0$  mm, and thickness  $W = 0.2$  mm. The thickness of Mylar film is  $G = 25$   $\mu\text{m}$ . All of the slits are infiltrated with LC E7, which is homeotropically aligned, as exhibited in the inset.

The finite element solver (COMSOL) is utilized to simulate the performances of the proposed filter. As stainless steel can be considered as a perfect electric conductor in the THz band, we set the relative permittivity of the stainless steel as 1 and the conductivity as  $1.6 \times 10^7$  ( $\Omega\text{m}$ )<sup>-1</sup> in

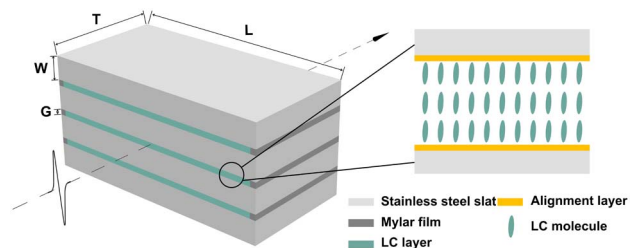


Fig. 1. Schematic structure of the proposed pseudo FP THz filter.

our calculations<sup>[12]</sup>. When a transverse magnetic (TM) wave is normally incident to the filter as shown in Fig. 1, surface plasmon polaritons (SPPs) are excited on both surfaces of each slat. The fields propagating along two adjacent interfaces couple together and concentrate in the LC layers<sup>[28–30]</sup>. The pitch of the structure ( $G + W$ ) is much less than the incident wavelength, therefore no diffraction occurs. On the other hand, the distance between neighboring slits ( $W = 0.2$  mm) is long enough to dissipate all of the laterally propagating SPPs, thus the coupling among different slits should be neglected. As a result, the component works as a pseudo FP cavity with reflecting front and rear interfaces.

If the incident wavelength  $\lambda_0$  satisfies  $\lambda_0 = 2nT/N$ <sup>[31]</sup>, standing waves of coupled SPPs are formed in the LC-filled slits. Here,  $N$  is the number of nodes and  $n$  is the effective refractive index for the given wavelength within the slits. The transmissions reach their maxima when SPP standing waves form in the slits. The calculated transmission spectra are shown in Fig. 2. The separate sharp peaks agree with the intrinsic property of FP resonance. The red solid line indicates the original state when  $n = 1.71 - 0.051i$ , which is about the extraordinary complex refractive index  $n_e$  of E7 at room temperature<sup>[32,33]</sup>. The black dashed line depicts the case at  $n = 1.62 - 0.03i$ , which is the isotropic complex refractive index  $n_{iso}$ . Here, the wavelength dispersion of the refractive index of LC is not considered as it is negligible in the range of 0.1–0.5 THz. As the absorption of LC increases along with the increase of frequency, the transmission decreases for the individual spectra. When the complex refractive index changes from  $n_e$  to  $n_{iso}$ , the overall transmission decreases due to the larger imaginary part of  $n_{iso}$ . The shift of the FP resonance frequency between the two spectra vividly reveals the tunability of the pseudo FP filter.

In our experiment, polyimide films are coated on both surfaces of the metal slats to carry out homeotropic alignment. Then, they are stacked together and sealed with a glue to form the designed structure. After infiltrated with LC E7, the component is fabricated. A THz time-domain spectroscopy (TDS) system is used to detect the transmission spectra of the filter. When the temperature increases,

the effective refractive index changes from  $n_e$  to  $n_{iso}$ , approximately. The spectra presented in Fig. 3 show the frequency-dependent transmission of the filter at different temperatures in the range of 25°C–85°C. Both the number of resonant transmission peaks and the shift range for given peaks are consistent with the simulated results. As expected, all peaks shift toward higher frequencies due to the continuous changing of  $n$  caused by increasing temperature. The obtained transmission is slightly lower compared to the simulation values due to scattering loss caused by the roughness of the rear and front interfaces of the real sample. The peak broadening is attributed to the nonuniformity of the lengths of the FP cavities, which determines the peak positions. The final obtained peak is a superposition of several separate ones, making the peak wider. Moreover, the transmission reduces in the temperature increasing process because the absorption loss caused by the LC layers rises<sup>[32,33]</sup>.

To clearly present the tunability to a given peak, we depict the dependency of a specific peak position on temperature in the range of 0.30–0.35 THz. As shown in Fig. 4, a total shift of up to 20 GHz is achieved, owing to the refractive index changing from  $n_e$  to  $n_{iso}$ , when the temperature varies from 30°C–80°C. In the range of 30°C–55°C, the peak position changes very slowly. After 55°C, a drastic change is observed as a drop of effective refractive

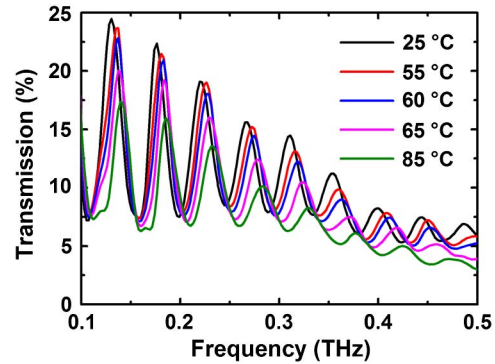


Fig. 3. Frequency dependent transmission of the filter at different temperatures.

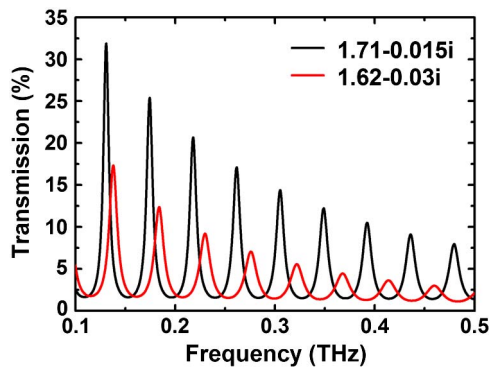


Fig. 2. Simulated transmission spectra of the designed filter with  $n = 1.71 - 0.015i$  and  $1.62 - 0.03i$ , respectively.

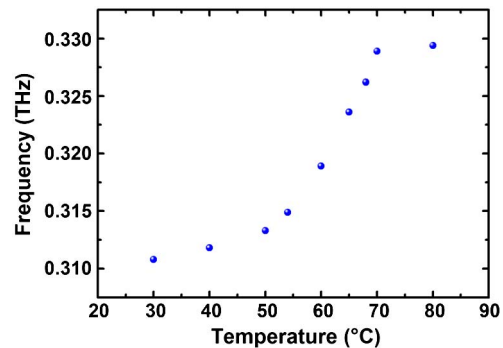


Fig. 4. Dependency of a specific peak position on temperature in the range of 0.30–0.35 THz.

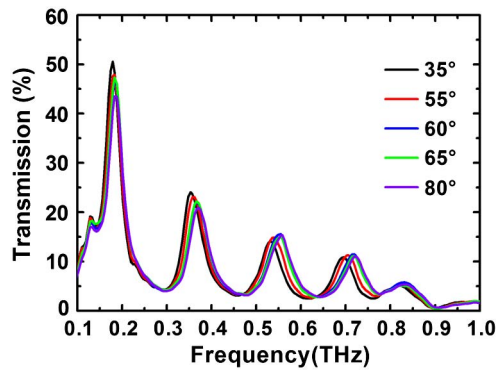


Fig. 5. Frequency-dependent transmission of the filter fabricated via precise laser processing at different temperatures.

index occurs around the clearing point of E7. No obvious shift is observed when the temperature exceeds 70°C. The shift of the peak position is coincident with the thermally induced refractive index change, verifying the thermal tunability of the proposed THz filter.

The performance of the filter could be tailored by changing the geometric parameters. A sample with dimensions of  $L = 10.0$  mm,  $T = 0.5$  mm,  $W = 0.15$  mm, and  $G = 25$   $\mu\text{m}$  was fabricated out of stainless steel slat by precise laser processing. After being immersed in a homeotropic alignment agent, LC E7 was infiltrated into the slits. Compared to the spectra in Fig. 3, the obtained transmittance here is increased, as shown in Fig. 5. The improvement is attributed to the reduced absorption loss in a shorter cavity. The peak position also shifted to a high frequency as the temperature increased from 35°C–80°C. Due to the restriction of laser processing, the thickness of the slats (i.e., the length of the cavity) is quite limited, making the peak distance very large. However, thanks to the good flexibility of the structure design and fabrication, the electric control of the orientation of the LC with a larger index change from  $n_e$  to  $n_o$  is achievable. Therefore, wider and more convenient tuning of the generated THz peaks could be realized.

In conclusion, we propose and demonstrate a tunable pseudo FP filter in the THz frequency range of 0.1–0.5 THz. It consists of alternative LC layers and metallic slats. By varying the refractive index of the filled LC via temperature control, the selective transmission frequencies are effectively tuned. The experimental results are consistent with simulations. A similar tunable filter is demonstrated by precise laser processing as well. The work supplies a novel design for tunable THz filters and brings new insights to the LC-based THz components of great potential in wide applications.

This work was supported by the National Natural Science Foundation of China (Nos. 11304151, 61490714, 61435008, and 61575093), the Ph.D. Programs Foundation of the Ministry of Education of China (No. 20120091120020), and the Fundamental Research Funds for the Central Universities (Nos. 021314380020

and 021314380023). The authors thank Gao-Chao Zhou and Prof. Biao-Bing Jin for their support on THz-TDS measurement, Zhao-Xian Chen for his constructive discussion, and Shao-Cheng Yan for his assistance on drawing the scheme.

## References

1. B. Ferguson and X. C. Zhang, *Nat. Mater.* **1**, 26 (2002).
2. M. Tonouchi, *Nat. Photonics* **1**, 97 (2007).
3. S. Koenig, D. Lopez-Diaz, J. Antes, F. Boes, R. Henneberger, A. Leuther, A. Tzschernig, R. Schmogrow, D. Hillerkuss, R. Palmer, T. Zwick, C. Koos, W. Freude, O. Ambacher, J. Leuthold, and I. Kallfass, *Nat. Photonics* **7**, 977 (2013).
4. J. Xu and X. C. Zhang, *Appl. Phys. Lett.* **88**, 151107 (2006).
5. D. Burghoff, T.-Y. Kao, N. Han, C. W. I. Chan, X. Cai, Y. Yang, D. J. Hayton, J.-R. Gao, J. L. Reno, and Q. Hu, *Nat. Photonics* **8**, 462 (2014).
6. S. G. Razavipour, E. Dupont, C. W. I. Chan, C. Xu, Z. R. Wasilewski, S. R. Laframboise, Q. Hu, and D. Ban, *Appl. Phys. Lett.* **104**, 041111 (2014).
7. D. M. Wu, N. Fang, C. Sun, X. Zhang, W. J. Padilla, D. N. Basov, D. R. Smith, and S. Schultz, *Appl. Phys. Lett.* **83**, 201 (2003).
8. N.-H. Shen, M. Massaouti, M. Gokkavas, J.-M. Manceau, E. Ozbay, M. Kafesaki, T. Koschny, S. Tzortzakis, and C. M. Soukoulis, *Phys. Rev. Lett.* **106**, 037403 (2011).
9. X.-W. Lin, J.-B. Wu, W. Hu, Z.-G. Zheng, Z.-J. Wu, G. Zhu, F. Xu, B.-B. Jin, and Y.-Q. Lu, *AIP Adv.* **1**, 032133 (2011).
10. L. Wang, X.-W. Lin, W. Hu, G.-H. Shao, P. Chen, L.-J. Liang, B.-B. Jin, P.-H. Wu, H. Qian, Y.-N. Lu, X. Liang, Z.-G. Zheng, and Y.-Q. Lu, *Light Sci. Appl.* **4**, e253 (2015).
11. L. Cong, N. Xu, J. Gu, R. Singh, J. Han, and W. Zhang, *Laser Photonics Rev.* **8**, 626 (2014).
12. R.-H. Fan, Y. Zhou, X.-P. Ren, R.-W. Peng, S.-C. Jiang, D.-H. Xu, X. Xiong, X.-R. Huang, and M. Wang, *Adv. Mater.* **27**, 1201 (2015).
13. C. Y. Chen, C. L. Pan, C. F. Hsieh, Y. F. Lin, and R. P. Pan, *Appl. Phys. Lett.* **88**, 101107 (2006).
14. I. C. Ho, C.-L. Pan, C.-F. Hsieh, and R.-P. Pan, *Opt. Lett.* **33**, 1401 (2008).
15. S. Biber, A. Hofmann, R. Schulz, M. Collischon, J. Weinzierl, and L. P. Schmidt, *IEEE T. Microw. Theory* **52**, 2183 (2004).
16. C. Winnewisser, F. T. Lewen, M. Schall, M. Walther, and H. Helm, *IEEE T. Microw. Theory* **48**, 744 (2000).
17. I. H. Libon, S. Baumgartner, M. Hempel, N. E. Hecker, J. Feldmann, M. Koch, and P. Dawson, *Appl. Phys. Lett.* **76**, 2821 (2000).
18. H. Nemeč, P. Kuzel, L. Duvillaret, A. Pashkin, M. Dressel, and M. T. Sebastian, *Opt. Lett.* **30**, 549 (2005).
19. I.-C. Khoo and S.-T. Wu, *Optics and Nonlinear Optics of Liquid Crystals* (World Scientific, 1993).
20. S. T. Wu, U. Efron, and L. D. Hess, *Appl. Phys. Lett.* **44**, 1033 (1984).
21. C. Y. Chen, T. R. Tsai, C. L. Pan, and R. P. Pan, *Appl. Phys. Lett.* **83**, 4497 (2003).
22. R. Wilk, N. Vieweg, O. Kopschinski, and M. Koch, *Opt. Express* **17**, 7377 (2009).
23. N. Vieweg, N. Born, I. Al-Naib, and M. Koch, *J. Infrared, Millimeter, Terahertz Waves* **33**, 327 (2012).
24. F. Z. Yang and J. R. Sambles, *Appl. Phys. Lett.* **79**, 3717 (2001).
25. S. A. Jewell, E. Hendry, T. H. Isaac, and J. R. Sambles, *New J. Phys.* **10**, 033012 (2008).
26. X.-Z. Wang, Z.-F. Wang, Y.-K. Bu, Z. Liu, L.-J. Chen, G.-X. Cai, Z.-P. Cai, and J. M. Dawes, *IEEE Photonics Technol. Lett.* **26**, 1983 (2014).

27. N. K. Reay, J. Ring, and R. J. Scaddan, *J. Phys. E Sci. Instrum.* **7**, 673 (1974).
28. M. B. Sobnack, W. C. Tan, N. P. Wanstall, T. W. Preist, and J. R. Sambles, *Phys. Rev. Lett.* **80**, 5667 (1998).
29. F. Z. Yang and J. R. Sambles, *Phys. Rev. Lett.* **89**, 063901 (2002).
30. H. E. Went, A. P. Hibbins, J. R. Sambles, C. R. Lawrence, and A. P. Crick, *Appl. Phys. Lett.* **77**, 2789 (2000).
31. M. Born and E. Wolf, *Principles of Optics: Electromagnetic Theory of Propagation, Interference and Diffraction of Light* (Cambridge University Press, 1999).
32. C.-S. Yang, C.-J. Lin, R.-P. Pan, C. T. Que, K. Yamamoto, M. Tani, and C.-L. Pan, *J. Opt. Soc. Am. B* **27**, 1866 (2010).
33. H. Park, E. P. J. Parrott, F. Fan, M. Lim, H. Han, V. G. Chigrinov, and E. Pickwell-MacPherson, *Opt. Express* **20**, 11899 (2012).